scientific reports

Check for updates

OPEN

Impact of spring sea ice variability in the Barents–Kara region on the Indian Summer Monsoon Rainfall

Divya Sardana & Ankit Agarwal✉

The rapidly changing Arctic climate significantly influences global weather systems primarily through high latitude teleconnections. While the Arctic-midlatitude interaction is well documented, the linkages between Arctic and tropical systems, particularly the Indian Summer Monsoon Rainfall (ISMR) is still in the nascent phase. This study investigates the impact of spring (March–May) sea ice anomalies in the Barents–Kara (B–K) region on ISMR patterns from 1959 to 2021. By categorizing years based on low- and high-sea-ice covers, we identify distinct atmospheric circulation patterns that modulate monsoonal variability over India. In the low-sea-ice years, reduced ice cover over the B–K region induces negative summer sea level pressure anomalies, triggering cyclonic activity and initiating a southward-propagating Rossby wave train. This wave train exhibits a distinct ridge-trough-ridge-trough pattern from Europe to the Far East and the North Pacific, shifting the subtropical westerly jet southward. This displacement enhances subsidence, suppresses convection over the Indo-Gangetic Plain, and ultimately reduces the monsoon rainfall in this region. Conversely, high-sea-ice years exhibit a reversed circulation pattern, with negative geopotential height anomalies over the B–K region and a ridge over central Asia, promoting upper-level divergence and strengthening monsoonal convection. These findings reveal the critical role of springtime B–K sea ice in modulating summer atmospheric circulation and ISMR, highlighting the far-reaching impact of Arctic sea ce variability on tropical weather systems.

Keywords Arctic, Barents–Kara sea, Indian summer monsoon rainfall, Composite analysis

The rapid warming of the Arctic has led to a phenomenon known as Arctic Amplification, where temperatures in the region increase at a rate significantly higher than the global average[1]. This accelerated warming is largely driven by positive feedback loops, such as the ice-albedo effect, water vapor feedback, and lapse rate feedback[2]. As sea ice cover diminishes, the reflectivity (albedo) of the Earth's surface decreases, leading to enhanced absorption of solar radiation by the ocean, which in turn accelerates warming[3]. Additionally, the reduction in sea ice weakens the temperature gradient between the polar and tropical regions, disrupting the atmospheric circulation patterns that have traditionally governed weather systems globally[4]. This shift in the temperature gradient is particularly important because it influences the dynamics of the jet stream and Rossby waves, leading to more persistent and extreme weather events in the tropics[5]. Consequently, gaining deeper insights into the influence of Arctic sea ice variability on large-scale atmospheric patterns and its downstream impacts on tropical weather systems is of critical importance.

Several studies have well-established that the decline in Arctic sea ice has a profound influence on mid-latitude weather patterns, which often contributes to colder conditions across northern continents[6], influences winter atmospheric blocking events (such as Ural blocking) and modulates weather patterns over Europe and Asia[7]. Melting Arctic sea ice can also disrupt ocean circulation, affecting weather in Europe and North America by slowing the Atlantic Meridional Overturning Circulation (AMOC)[8]. In particular, sea ice loss in the Barents–Kara (B–K) sea has been linked to alterations in the polar vortex and stratospheric circulation, which are critical drivers of mid-latitude climate variability[9].

Beyond mid-latitude impacts, recent research highlights the role of Arctic sea ice loss in shaping tropical climate systems. For instance, the retreat of Arctic sea ice has been associated with equatorward shifts in the Intertropical Convergence Zone (ITCZ), leading to warming in the tropical upper troposphere[10]. Additionally, numerical model simulations suggest that Arctic sea ice fluctuations significantly affect the Hadley circulation and equatorial Pacific Sea Surface Temperatures (SSTs), indicating potential global climate repercussions[11,12].

Department of Hydrology, Indian Institute of Technology, Roorkee, Uttarakhand 247667, India. ✉email: ankit.agarwal@hy.iitr.ac.in; agarwal.10891.ankit@gmail.com

Studies also report the impact of spring Arctic sea ice on the East Asian Summer Monsoon via teleconnections involving North Pacific SSTs[13]. Furthermore, early-winter sea ice conditions in the Laptev Sea have been associated with variations in the Indian Ocean Dipole (IOD), which in turn impacts the Indian Summer Monsoon Rainfall (ISMR)[14].

The emerging literature reveals growing interest in examining the teleconnections between the Arctic and tropical regions, with a particular emphasis on understanding how Arctic sea ice variability affects the ISMR. For instance, Kulkarni and Agarwal highlight the pronounced link between Arctic sea ice extent and Indian precipitation, emphasizing the importance of further exploring these teleconnections[15]. Recently, their study demonstrated that Arctic sea ice concentration (SIC) variability in the Atlantic and Pacific sectors influences ISMR patterns through the North Atlantic Oscillation (NAO) and El Niño Southern Oscillation (ENSO)[16]. While Zhu et al. explored the reverse dynamic, showing that ISMR modulates Arctic sea ice thickness by altering longwave radiation, independent of ENSO events[17]. These studies underscore the complex bi-directional interactions between the Arctic and Indian monsoon systems.

Such interactions are further amplified by the consequences of Arctic sea ice loss, which alters large-scale atmospheric circulation, modifying Rossby wave propagation and shifting the subtropical jet stream. These changes can significantly affect the ISMR onset and intensity[14,18]. Furthermore, Arctic changes influence the IOD and Madden-Julian Oscillation (MJO), both critical drivers of ISMR variability[11,13]. As climate change accelerates Arctic sea ice decline, understanding these complex linkages is crucial for improving seasonal monsoon forecasting and mitigating potential socio-economic impacts across the Indian subcontinent.

Previous studies have shown that October sea ice extent in the B–K sea is closely linked to the following summer's monsoon rainfall over India, where lower sea ice extent tends to weaken monsoon activity, and higher extent is associated with stronger monsoons[19]. Besides, the retreat of sea ice in the Kara–Laptev Seas has been associated to an increase in late-season, high-intensity rainfall events over India[20]. The B–K region, situated to the northwest of Russia, plays a pivotal role in shaping Arctic climate dynamics. This region has been increasingly influenced by the northward expansion of warm Atlantic Ocean waters, a phenomenon known as "*Atlantification*"[21]. The anomalous inflow of these warm, saline water disrupts ocean stratification and ventilation, leading to enhanced meridional heat flux and vertical mixing[22]. These changes are further sustained by shifting atmospheric storm tracks and winds as well as various radiative and climate feedback processes[23,24].

Research indicates that sea ice anomalies in the B–K region significantly influence atmospheric circulation patterns, including stratosphere-troposphere coupling[25,26]. These atmospheric responses have the potential to extend beyond the polar regions, impacting tropical weather systems[2,27,28]. Despite the well-established role of Arctic sea ice in influencing global and regional climate, the specific impacts of springtime sea ice variability in the B–K sea, often termed as the "*Arctic warming epicenter*" on the ISMR, remain underexplored[29,30]. Hence, this study addresses this critical research gap by systematically analyzing the mechanisms through which spring SIC anomalies in the B–K region drive changes in monsoon dynamics over India. By employing a composite analysis of low- and high-sea-ice years, this research provides novel insights into the broader teleconnections between Arctic sea ice conditions and tropical climate variability that modulate changes in large-scale atmospheric circulation patterns and associated teleconnection mechanisms, subsequently influencing the variability of ISMR.

Materials and Methods

Study Area and Datasets

The Arctic, located above 66.5° N latitude, encompasses the Arctic Ocean, which is surrounded by key landmasses and divided into several marginal seas (Fig. 1a). These include the Greenland, Barents, Kara, Laptev, and East Siberian Seas near the Eurasian continent, as well as the Beaufort, Baffin Bay, and Chukchi Seas near the North American continent. The Arctic Ocean connects to the Pacific Ocean via the Bering Strait and to the Atlantic Ocean through the Greenland and Labrador Seas[31]. Among these marginal seas, the B–K region (20° E–90° E, 65° N–85° N; outlined in black dotted lines in Fig. 1a) has gained increasing attention in recent years due to a significant decline in sea ice, with studies highlighting its amplified warming compared to other Arctic regions[32,33]. The growing recognition of the B–K region's central role in driving large-scale atmospheric changes underscores its selection for this study.

To assess the possible association between springtime (March–May) sea ice anomalies in the B–K region and ISMR, this study relies on SIC data obtained from the ERA5 reanalysis (the fifth generation of ECMWF) spanning from 1959 to 2021. ERA5 is selected due to its long-term availability and advanced data assimilation techniques, offering high spatial (0.25° × 0.25°) and temporal (hourly) resolution. Large-scale oceanic and atmospheric circulation patterns are also analyzed using key variables, including SST, 2-meter air temperature, sensible heat flux, mean sea level pressure (MSLP), wind speed (200 hPa and 850 hPa), and geopotential height (200 hPa and 850 hPa), zonal wind anomaly at 10 hPa. The zonal-mean of the zonal wind at 10 hPa (~ 30 km) and 60°N, which is the westerly wind during winter, is commonly used to detect the strength of the stratospheric polar vortex. To better understand the plausible physical mechanisms linking the B–K region to monsoonal variability, additional variables such as vertical velocity (500 hPa), divergence (500 hPa), and Convective Available Potential Energy (CAPE) were considered. All datasets were sourced at a 6-hourly resolution to capture detailed atmospheric variability and converted into seasonal data using the Climate Data Operator (CDO).

In India, the ISMR is responsible for over 80% of the country's annual rainfall[35]. Precipitation patterns exhibit considerable spatial and temporal variability, with the monsoon season being the key period of rainfall. The country is divided into six homogeneous rainfall regions based on these patterns: Northwest, Northeast, Central Northeast, West Central, Peninsular, and the Hilly region (Fig. 1b;[36]. For the investigation of ISMR, we use daily gridded rainfall data at a 0.25° × 0.25° resolution, spanning 1959 to 2021, sourced from the India Meteorological Department (IMD). This dataset, generated from over 6,000 gauging stations across India, has been widely

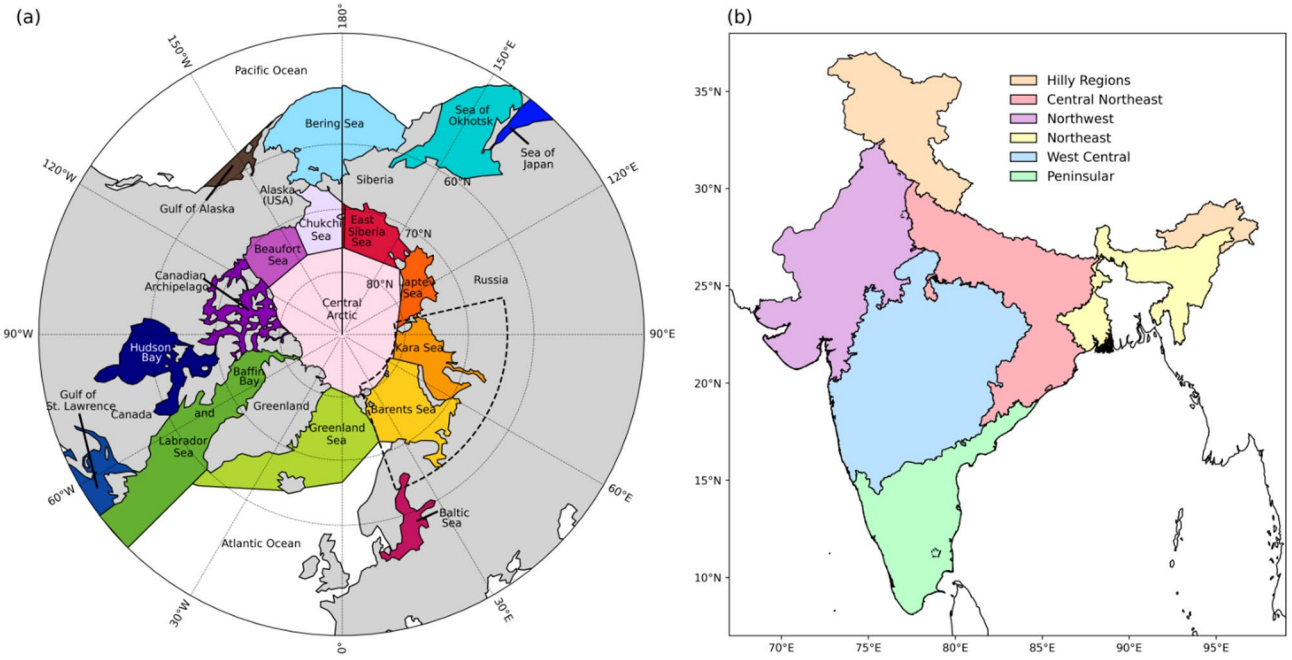

Fig. 1. Study area and regional classification (**a**) Map of the Arctic Ocean showing its sub-regions. The Barents and Kara Seas (20° E–90° E, 65° N–85° N) are outlined with dotted lines, representing the domain used to produce the sea ice concentration index in this study (**b**) Homogeneous regions of India based on rainfall patterns. Figure adopted and modified from[34]. The map was generated using Python version 3.12 and is available at https://www.python.org/.

used in various hydroclimatic studies to capture the detailed characteristics of the ISMR, including its seasonal distribution and orographic effects in the Western Ghats and the Himalayas[37]. The seasonal mean and maximum rainfall are derived from daily datasets and are referred to as mean and extreme ISMR, respectively.

Methodology

The study employs composite analysis to examine the impact of B–K sea ice anomalies on ISMR patterns. As a first step, an area-averaged SIC index is constructed for the B–K region during the spring season. To eliminate long-term trends, ensure consistency, and isolate the interannual variability, the SIC time series is first detrended by computing and subtracting its linear trend. The resulting series is then standardized to have zero mean and unit standard deviation (see Fig. S1a), enabling uniform comparison across the study period. Fig. S1b depicts the correlation between the absolute sea ice index and ISMR, indicating a significant relationship between Arctic sea ice variability and ISMR. However, to better understand the contrasting atmospheric responses, it is necessary to examine the segregated impacts during low- and high-ice years. Years with standardized SIC anomalies exceeding + 1 standard deviation are classified as "high sea ice" years, while those falling below − 1 standard deviation are categorized as "low sea ice" years. Based on this classification, the identified low sea ice years are 1964, 1965, 1973, 1975, 1992, 1995, 2006, 2007, 2012, and 2016. The corresponding high sea ice years are 1966, 1969, 1978, 1979, 1981, 1982, 1987, 1998, 1999, and 2003.

Composite analysis, also referred to as conditional sampling, is a widely used statistical technique in climate science that helps isolate robust signals associated with specific events or conditions while minimizing unrelated background variability. Originally introduced by Chree et al. in space science, composite analysis has since found broad applications in Earth system studies[38–41]. The method involves identifying a set of key events, typically defined as positive or negative phases of an index (here, high/low SIC), and then computing the average of a climate variable over the time steps associated with those events. This procedure enhances recurring patterns associated with the events while noises are averaged out.

In this study, composite analysis is conducted for the June–September (JJAS) season, which marks the peak of the ISMR. Years with anomalously low and high Arctic SIC in the preceding spring are identified as the key events. Composite anomalies for key variables mentioned in the Data section are calculated as deviations from the JJAS climatological mean over the full study period. This enables us to examine how springtime sea ice conditions may modulate large-scale atmospheric circulation and impact monsoon rainfall across the Indian subcontinent. Also, to examine the large-scale circulation response, streamfunction anomalies were computed from wind speed components and geopotential height fields following the formulation of Takaya and Nakamura[42].

Results

Composite analysis of ISMR response to Arctic sea ice variability

The composite analysis of mean and extreme ISMR anomalies during low- and high-sea-ice years spanning 1959 to 2021 is illustrated in Fig. 2. During low sea ice years, the Indo-Gangetic Plain, a crucial agricultural and densely populated region (outlined in black dotted lines in Fig. 2a), exhibits widespread negative mean rainfall anomalies, indicating weakened monsoon activity. The Indo-Gangetic Plain, also known as the Northern Plain, is a fertile plain spanning the northern and north-eastern part of the Indian subcontinent and is well known for its agricultural productivity. This reduction in rainfall over this region aligns with a weakened monsoon trough and a diminished land-sea thermal gradient, as reported in previous studies[43]. However, during these years, positive mean ISMR anomalies are observed across much of India, including Rajasthan, Vishakhapatnam, Nagpur, the Western Ghats, parts of the western Himalayan and northeastern India, suggesting a regional redistribution of rainfall[44,45]. These anomalies may be associated with localized convective activity and shifts in monsoonal wind patterns, thereby underscoring the complex interactions between Arctic forcing and regional climatic responses over India.

Conversely, during high sea ice years (Fig. 2b), enhanced monsoon activity is evident, particularly over the Indo-Gangetic Plain and parts of northeast India, where positive mean ISMR anomalies reach up to 140 mm.

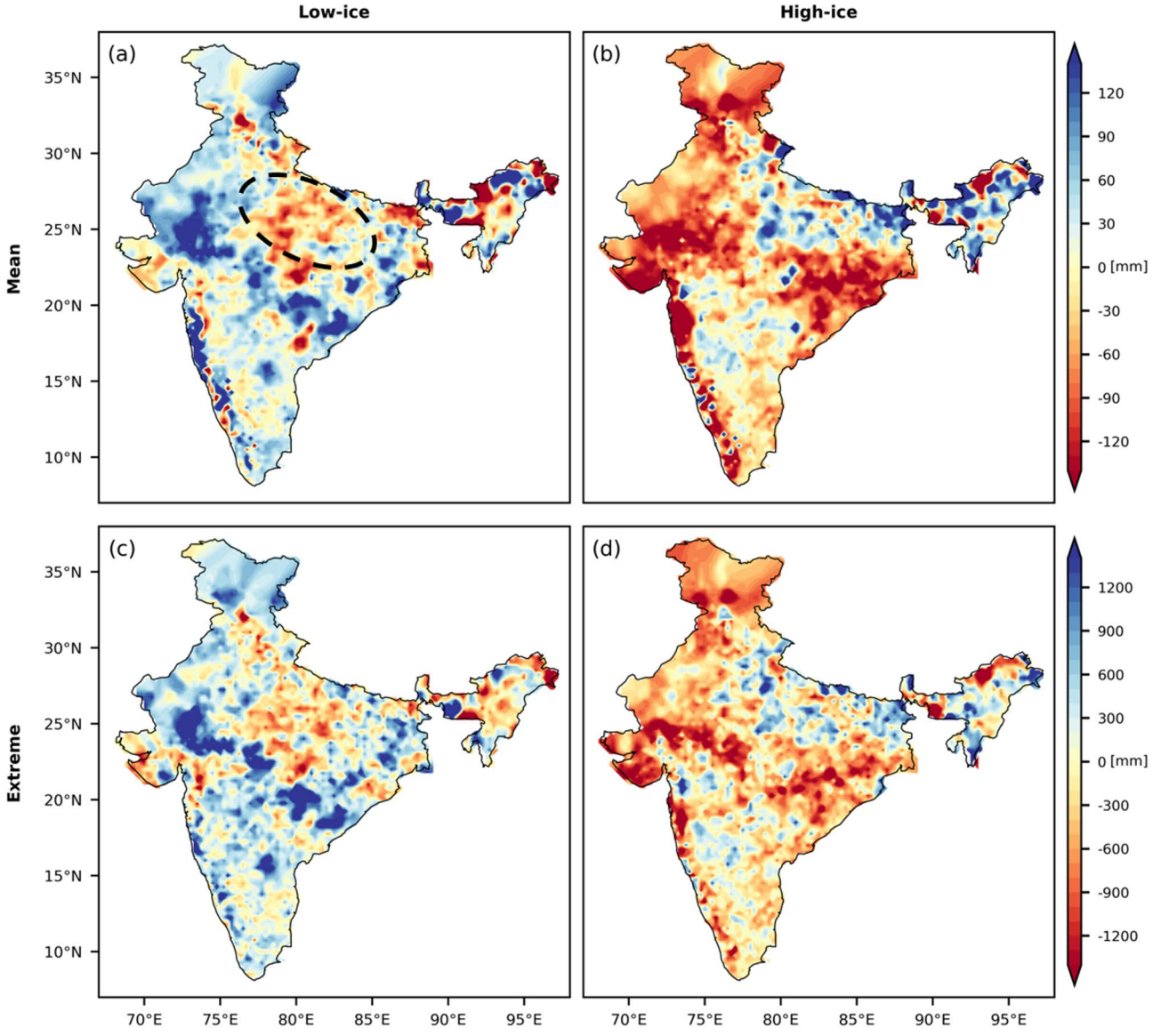

Fig. 2. Evolution of Indian Summer Monsoon Rainfall associated with low and high sea ice years spanning 1959 to2021. Composite anomalies of (**a**) mean and (**c**) extreme rainfall during low sea ice years (**b**) Same as (**a**) but for high sea ice years (**d**) Same as (**c**) but for high ice years. Here, mean and extreme rainfall refer to the seasonal mean and maximum rainfall, respectively. Low and high sea ice years are identified based on spring (MAM) sea ice index over the Barents–Kara region, while all rainfall anomalies are computed for the JJAS season. Black dotted lines mark the Indo-Gangetic region in panel (**a**).

This increased rainfall is linked to a strengthened monsoon trough and enhanced low-level jet activity, which facilitates moisture advection from the Arabian Sea and the Bay of Bengal[46,47]. In contrast, regions such as the Western Ghats, northern, western, and southeast India exhibit pronounced negative mean ISMR anomalies, potentially linked to large-scale subsidence and atmospheric divergence, induced by intensified convective activity in adjacent areas[48]. Extreme ISMR anomalies during low and high ice years follow a similar pattern but with ten times greater intensity, ranging from −1200 to 1200 mm (Fig. 2c, d). This illustrates the significant impact of sea ice variability on extreme rainfall events as well.

Overall, low (high) sea ice years are predominantly associated with reduced (enhanced) rainfall across the Indo-Gangetic plain. The pronounced contrast in ISMR anomalies during low- and high-sea-ice years suggests a strong teleconnection between springtime B–K sea ice variability and the ISMR. Sea ice variability in this region influences large-scale oceanic and atmospheric circulation patterns (discussed in the following sub-sections), such as planetary wave propagation, subtropical jet shifts, and mid-latitude westerlies, which, in turn, affect the strength and position of the monsoon trough over the Indian subcontinent[2,49,50]. Studies have shown that Arctic Amplification can further enhance these teleconnections, altering the jet stream and Rossby waves, leading to significant changes in monsoon patterns[51].

To investigate the statistical consistency of the proposed mechanisms, a cross-correlation analysis was performed between SIC, SST, near-surface air temperature, MSLP, geopotential height at 200 hPa and 850 hPa, and ISMR (Fig. S2). The analysis reveals a robust negative relationship between SIC and SST ($r = -0.95$), and SIC and near-surface air temperature ($r = -0.84$), highlighting strong surface thermodynamic coupling. In addition, strong positive correlations between upper- and lower-tropospheric geopotential heights ($r \approx 0.95$) and their moderate associations with MSLP suggest a vertically coherent atmospheric adjustment that links surface anomalies to large-scale circulation. These results provide concrete statistical evidence that the observed SIC anomalies are systematically connected with both surface and upper-level atmospheric fields, thereby lending statistical support to the teleconnection mechanisms proposed in this study. A more detailed examination of these relationships is carried out in the following subsections using composite analysis of the relevant climate variables.

Composite analysis of thermal and pressure anomalies

This section examines the composite anomalies of SST, 2-meter air temperature and SLP during low and high sea ice years (see Fig. 3). During low sea ice years, pronounced warm SST anomalies are observed over the B–K sea, followed by Laptev Sea, Beaufort Sea, Canadian Archipelago, Baffin Bay and Labrador Sea (Fig. 3a). This warming is a manifestation of Arctic Amplification, a process in which the Arctic experiences enhanced warming compared to lower latitudes due to multiple feedback mechanisms. A key contributor in the B–K region is Atlantification, driven by increased intrusion of warm Atlantic waters, which reduces sea ice cover, disrupts ocean stratification, and alters ocean-atmosphere fluxes[52,53]. As sea ice retreats, the lower albedo of open water enhances, reinforcing regional warming and sustaining feedback loops[3]. This intensified warming weakens the meridional temperature gradient and disrupts atmospheric circulation. Studies suggest it can alter the strength of the westerlies and shift storm tracks, potentially affecting circulation patterns like the NAO and the jet stream[50].

Similar to SST, 2m air temperature anomalies exhibit a pronounced warming signal over the Arctic during low ice years (Fig. 3b). The strongest warming is concentrated over the B–K Sea, Laptev Sea, and Beaufort Sea, where temperature anomalies exceed 0.5°C. This atmospheric warming is primarily driven by the release of heat from the ice-free ocean surface into the lower troposphere, reinforcing the Arctic Amplification process. Additionally, warm anomalies extend beyond the Arctic, reaching northern Eurasia and parts of North America, highlighting the broader climatic implications of Arctic sea ice loss. This extensive warming can influence large-scale atmospheric circulation patterns, modulating the strength and position of the polar jet stream and mid-latitude weather systems. According to the thermodynamic principle, this warming leads to lower surface pressure because warm air is less dense than cold air, and as a result, it rises, creating a region of lower pressure at the surface. Hence, as evident from Fig. 3 (c), the Arctic region exhibits negative SLP anomalies during low ice years in summer, with the most pronounced anomalies observed in the B–K sea.

In contrast, during high sea ice years, cooler SST anomalies dominate the Arctic and adjacent high-latitude regions, with pronounced anomalies over the B–K sea, Laptev Sea, East Siberia Sea (Fig. 3d). Enhanced sea ice cover increases surface albedo, reducing solar heat absorption and limiting ocean-atmosphere heat exchange[54]. These cooler-than-average conditions result from reduced atmospheric heat transport, and a weakened pole-to-equator temperature gradient. Correspondingly, 2m air temperature anomalies (Fig. 3e) show widespread cooling, especially over regions of extensive sea ice. This reinforces feedback between sea ice, surface temperature, and circulation. The SLP anomalies (Fig. 3f) show high pressure over the Arctic and low pressure over the North Pacific, Norway, Sweden, and Finland. Together, panels 3d–f highlights the strong coupling between Arctic Sea ice variability and atmospheric circulation, with broader implications for high-latitude and tropical climate systems.

Further, the sensible heat flux (SHF) composites reveal strong upward anomalies along the Barents–Kara margins during high-ice years, while low-ice years are characterized by weaker and spatially diffuse anomalies (Fig. S3a, b). This contrast indicates that the magnitude of surface–atmosphere heat exchange depends strongly on the background sea ice state. SHF anomalies provide localized energy input into the lower troposphere, which can act as a potential precursor for planetary wave excitation and downstream circulations.

Atmospheric circulations associated with low and high ice years

The influence of Arctic sea ice variability on atmospheric circulation extends beyond thermal and pressure anomalies. These changes propagate into the upper and lower troposphere, altering geopotential height (GPH)

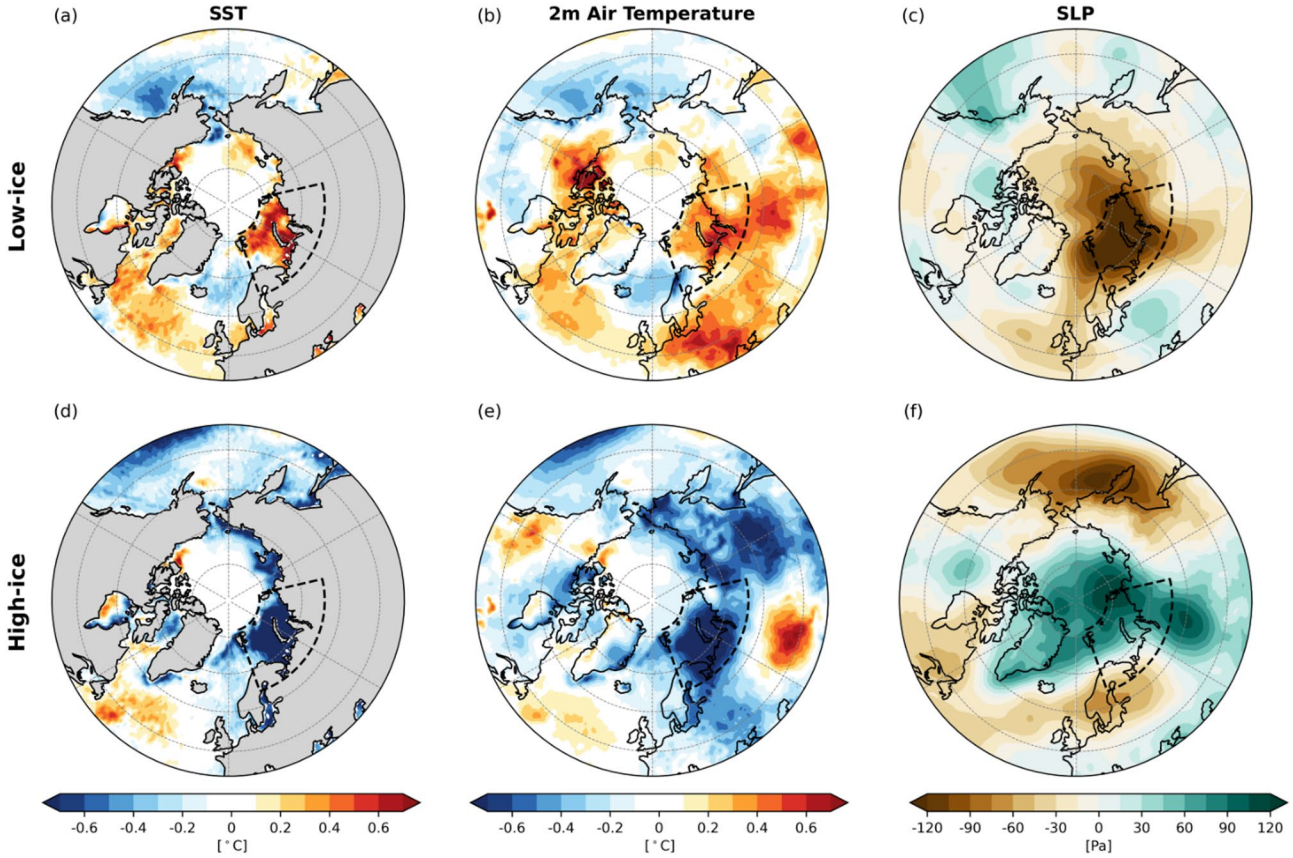

Fig. 3. Evolution of thermal and pressure anomalies during the spring season associated with low and high sea ice years spanning 1959–2021. Composite analysis of (**a**) sea surface temperature (SST), (**b**) 2-meter air temperature, and (**c**) sea level pressure (SLP) during low sea ice years. Panels (**d**), (**e**), and (**f**) show the corresponding anomalies for high sea ice years, respectively. Dotted lines in each panel represent the Barents–Kara region.

at different pressure levels, which plays a crucial role in modulating large-scale atmospheric circulation, and subsequently the ISMR. To understand this connection, we examined composite anomalies of GPH and associated wind speed at 200 hPa and 850 hPa (Fig. 4). At 200 hPa, GPH anomalies reflect variations in the distribution of atmospheric mass and pressure in the upper troposphere, with ridges (high-pressure systems) and troughs (low-pressure systems) shaping large-scale circulation patterns. These features modulate the subtropical westerly jet stream (SWJ) and the tropical easterly jet (TEJ), both of which play a critical role in monsoonal dynamics.

The SWJ, located in the midlatitudes (Fig. S4a), is a fast-flowing, narrow air current in the upper troposphere that governs the movement of synoptic systems, including mid-latitude troughs and ridges[55]. A weakening of the SWJ is often associated with a delayed monsoon onset over India. In contrast, the TEJ is a dominant upper-level easterly wind system that emerges over the Indian Ocean, extends across South Asia during JJAS, and enhances upper-level divergence over the Indian subcontinent (Fig. S4a). It is established due to the meridional temperature gradient between the equatorial Indian Ocean and the Asian landmass, and extends from the Pacific Ocean to the west coast of the Sahel. Elevated heating over the Tibetan Plateau increases this gradient and leads to an enhancement of the TEJ[56].

During low ice years (Fig. 4-Panel I), negative GPH anomalies (200 hPa) dominate the Arctic and extend downstream over Eurasia, indicating a weakened polar vortex and enhanced cyclonic circulation (Fig. 4a). This weakened vortex disrupts the typical jet streams, amplifying the Rossby wave activity, hence creating a ridge-trough-ridge-trough wave train pattern in the latitudinal band of 50°N-65°N. The deepened trough over central Eurasia not only influences the mid-tropospheric circulation but also interacts with the South Asian monsoon system. These GPH patterns are accompanied by the weakened and southward displaced subtropical jet stream. This enhances subsidence (sinking motion) over the Indo-Gangetic plain, which limits the strength of vertical air-motion needed for convection in this region. At 850 hPa, southwesterly winds are evident (Fig. S4b), which are moisture-laden winds that originate in the Indian Ocean and move towards the Indian subcontinent during the monsoon season. During low-ice years, upper-level winds (200 hPa) remain weak (Fig. 4c), while strengthened wind anomalies are prominent across the Indo-Gangetic Plain at 850 hPa (Fig. 4d). This atmospheric configuration influences precipitation patterns in the region through the interplay of moisture transport, atmospheric stability, and vertical motion dynamics[43].

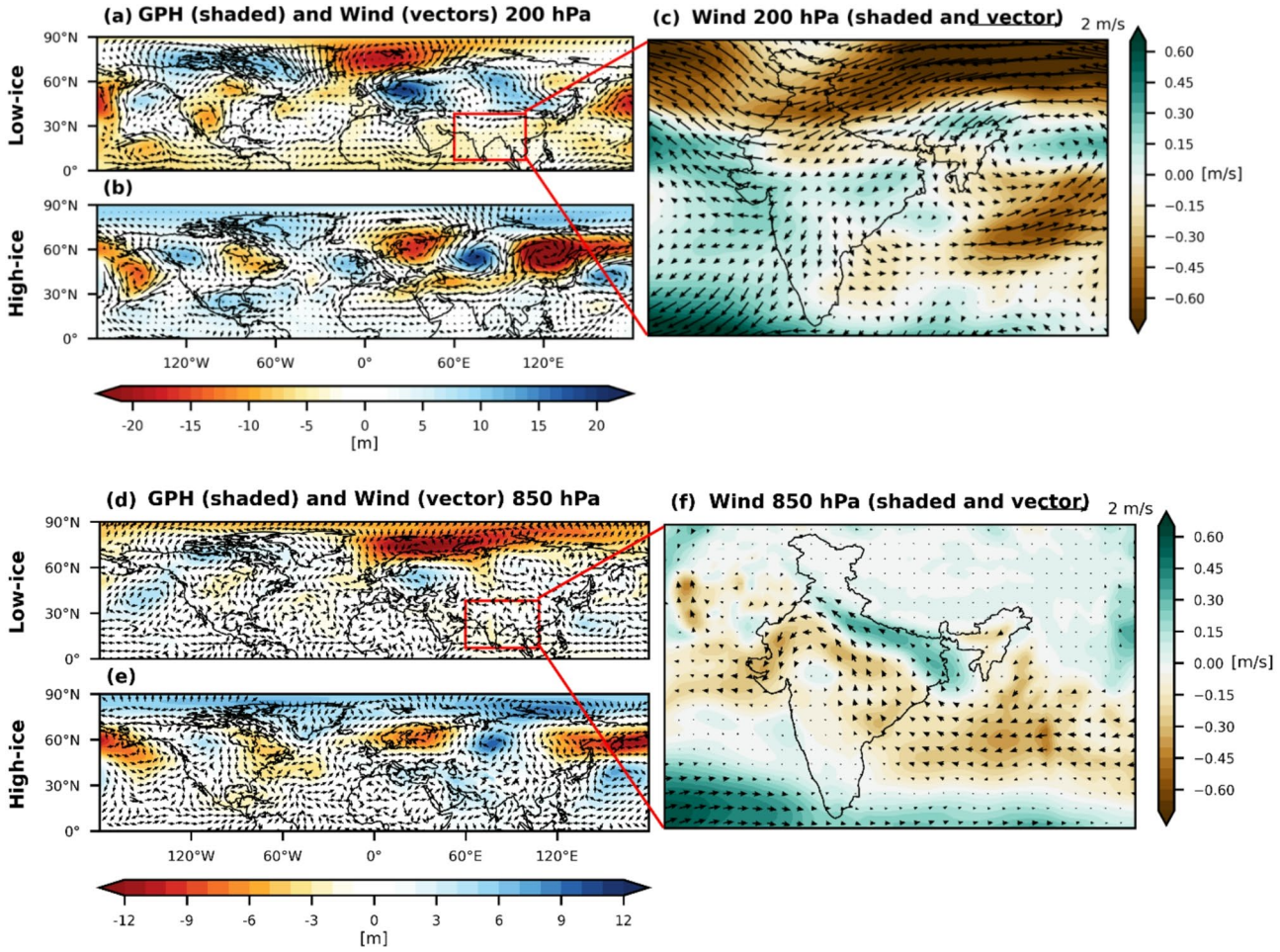

Fig. 4. Evolution of geopotential height and wind speed anomalies during the spring season associated with low and high sea ice years in the upper (200 hPa) and lower (850 hPa) troposphere (**a**) Composite anomalies of geopotential height (shaded) and wind speed (vectors) at 200 hPa during low sea ice years (**b**) Same as (a) but for high sea ice years (**c**) Wind speed anomalies (shaded and vectors) at 200 hPa during low sea ice years (**d**) Composite anomalies of geopotential height (shaded) and wind speed (vectors) at 850 hPa during low sea ice years (**e**) Same as (d) but for high sea ice years (**f**) Wind speed anomalies (shaded and vectors) at 850 hPa during low sea ice years. The geopotential height anomalies reveal a ridge–trough–ridge–trough wave train structure in the 50°N–65°N latitudinal band, indicative of enhanced Rossby wave activity during low sea ice years. Note that ridges and troughs represent the high- and low-pressure systems, respectively.

Enhanced winds at 850 hPa typically facilitate increased moisture transport into the region, supporting convective activity (Fig. 4f). However, when upper-level winds at 200 hPa are weak, they can suppress vertical air movement by promoting subsidence (sinking motion)[57]. This results in insufficient upper-level divergence, which is crucial for sustaining upward motion and deep convection. The weakened upper-level winds indicate reduced outflow from convective systems, limiting the development of intense precipitation events. The imbalance between lower-level moisture advection and upper-level stability creates a more stable atmosphere, inhibiting deep convective cloud formation and leading to a reduction in rainfall over the Indo-Gangetic Plain[58]. In contrast, during high-ice years, the atmospheric circulation exhibits an opposite configuration, thereby reversing the suppressed convection and supporting more favorable conditions for monsoonal rainfall across the Indo-Gangetic Plain (Fig. 4b, e).

Diagnostic analysis of regional atmospheric dynamics associated with Arctic sea ice variability

The variability in Arctic sea ice has the potential to modulate the ISMR through complex atmospheric processes involving changes in vertical motion, horizontal divergence and atmospheric instability. In this section, we present a diagnostic analysis of atmospheric conditions during contrasting sea ice states (low vs. high sea ice years) emphasizes key atmospheric variables that could mediate the Arctic to-topical linkages particularly over the Indo-Gangetic plain.

We first examined vertical atmospheric motion through a composite analysis of vertical velocity at 500 hPa level positioned between 200 hPa and 850 hPa levels during the monsoon season JJAS (Fig. 5a, d). During low ice

year, significant positive vertical velocity anomalies (enhanced subsidence) are observed over the Indo-Gangetic Plain (Fig. 5a), indicating that the atmosphere in the region is experiencing stronger-than-usual subsidence relative to the climatological baseline. Enhanced subsidence (marked by positive anomalies) inhibits convective uplift by stabilizing the atmospheric column, leading to warming and drying of descending air parcels, thus suppressing cloud formation and precipitation[43]. Such a pattern aligns well with reduced rainfall observed during low sea ice years. Conversely, high sea ice years display weaker subsidence or even ascent (negative anomalies), supporting enhanced convective activity and increased rainfall.

Horizontal divergence anomalies at 500 hpa during the JJAS season further support this interpretation (Fig. 5b, e). During the low sea ice years, positive divergence anomalies (blue) over the Indo-Gangetic Plain (Fig. 5b) indicate the dominance of the horizontal outflow at mid-levels, suppressing vertical uplift and convection[47]. These anomalies are particularly pronounced during low ice years, further supporting the role of subsidence in reducing rainfall. In contrast, high ice years (Fig. 5e) are characterized by negative divergence anomalies (convergence) which enhance vertical motion, fostering convective cloud development and thus promoting increased rainfall. This contrasting divergence behavior underscores the critical role of horizontal airflow dynamics in modulating regional monsoonal rainfall in response to Arctic variability.

Additionally, atmospheric instability, quantified by CAPE, exhibits clear differentiation between low and high sea ice conditions (Fig. 5c, f). CAPE quantifies the buoyancy and potential instability of atmospheric parcels[59,60]. During low-ice years, significant negative CAPE anomalies are observed over the Indo-Gangetic Plain (Fig. 5c), suggests that the atmosphere is more stable, with cooler air parcels that are less buoyant and unable to rise effectively. This increased stability inhibits convection, leading to reduced cloud formation and precipitation. Conversely, positive CAPE anomalies during high ice years (Fig. 5f) indicate greater atmospheric instability, which facilitates the development of convective clouds and enhances the likelihood of precipitation. This pattern further reinforces the connection between atmospheric stability and rainfall patterns, with low ice years linked to drier conditions and high ice years associated with enhanced rainfall over the Indo-Gangetic Plain.

Collectively, these diagnostic atmospheric variables (vertical velocity, divergence, and CAPE) illustrate distinct regional dynamics during contrasting sea ice scenarios. Although this analysis identifies key atmospheric conditions associated with sea ice anomalies, further research is needed to elucidate specific dynamical pathways or intrinsic modulators—such as changes in planetary wave activity, mid-latitude jet-stream dynamics, or land-atmosphere interactions—that physically mediate Arctic-to-ISMR teleconnections.

Discussion

This study demonstrates a pronounced relationship between springtime B–K sea ice variability and ISMR, thereby emphasizing the far-reaching teleconnections that couple high-latitude processes with tropical climate systems. During low sea ice years, reduced monsoon activity is observed across key agricultural regions such as

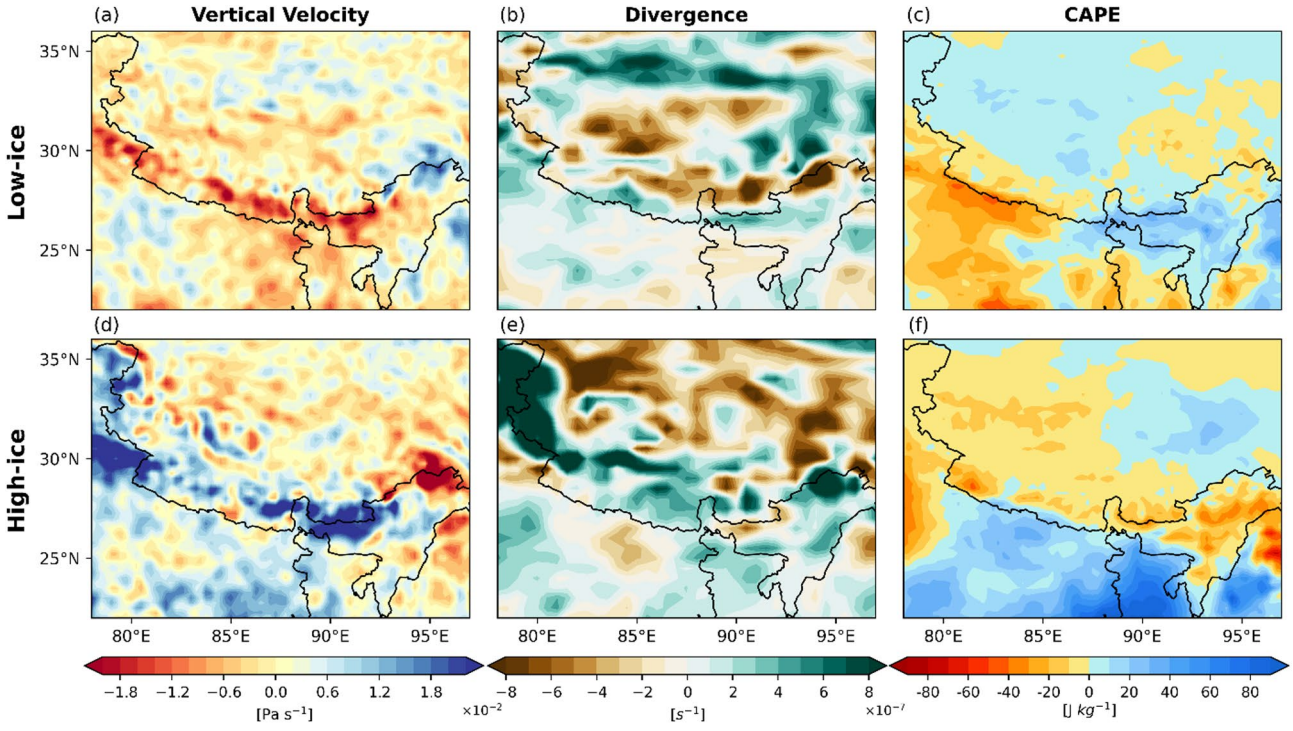

Fig. 5. Diagnostic indicators of regional atmospheric dynamics during the summer season associated with low and high sea ice years over the region 22°–36° N; 78°–97° E. Composite analysis of (**a**) vertical velocity (**b**) divergence, and (**c**) Convective Available Potential Energy (CAPE) anomalies at 500 hPa during low ice years. Panels (**d**), (**e**), and (**f**) show the corresponding anomalies for high sea ice years.

the Indo-Gangetic Plain, primarily due to the weakening of the monsoon trough and reduced land-sea thermal contrast. Conversely, high sea ice years depict an enhanced monsoon, particularly over the Indo-Gangetic Plain, driven by the strengthening of the monsoon trough and the low-level jet. This stark contrast in ISMR patterns emphasizes the influence of Arctic conditions on the tropics, further confirming the relevance of high-latitude processes in shaping tropical weather systems, a relationship that has been underexplored in regional studies[61].

Previous studies have examined the teleconnections between Arctic sea ice variability and monsoon dynamics, primarily focusing on East Asian climate patterns. Yang et al. demonstrated that reduced sea ice in the B–K Seas during early winter influences June precipitation in China through atmospheric wave propagation[62]. Similarly, Xu et al. found that sea ice decline in the B–K region deepens the East Asian trough, affecting wintertime precipitation patterns[63]. While these studies highlight the significant role of Arctic forcing on East Asian climate variability, the impact on the ISMR has been less extensively investigated. Our study fills this research gap by establishing a robust relationship between B–K sea ice variability and the ISMR, providing novel insights into Arctic-tropical climate interactions that influence monsoon variability over the Indian subcontinent.

The modulation of atmospheric circulation patterns by Arctic sea ice further underscores the intricate connections between polar and tropical climates, reinforcing the importance of high-latitude processes in regulating tropical weather systems. Studies have highlighted that Arctic warming, associated with sea ice decline, disrupts mid-latitude atmospheric circulation by weakening the westerlies and shifting storm tracks[3,64]. Our analysis supports these findings, demonstrating that Arctic warming during low ice years induces lower surface pressures across the Arctic, which subsequently modifies global atmospheric circulation. These changes manifest in geopotential height (GPH) anomalies, where negative GPH anomalies over Eurasia during low ice years correspond to a weakened polar vortex and enhanced cyclonic circulation. This disruption in mid-latitude circulation is consistent with previous findings[2], who linked Arctic Amplification to altered jet stream patterns and increased climate variability in the Northern Hemisphere.

In support of this, the streamfunction anomalies (Fig. 6a, b) reveal negative and positive anomalies over the B–K region during low and high ice years, respectively. This indicates contrasting wave propagation pathways downstream into Eurasia, and further influencing the large-scale circulation relevant for monsoon variability. As evident in Fig. 6c and d, wintertime polar vortex has a stronger tendency to weaken in years when Arctic sea ice is accelerating its disappearance, suggesting that the stratosphere-troposphere coupling provides an additional pathway through which the Arctic influences the tropical weather patterns and contributes to increased monsoonal variability.

Furthermore, our study highlights the role of large-scale atmospheric features such as the monsoon trough and the subtropical westerly jet (STWJ) in mediating the Arctic-ISMR connection. Previous research emphasized the importance of upper-level circulation anomalies in driving monsoon variability, noting that weakened STWJ patterns can lead to reduced convective activity and suppressed rainfall[65]. Our findings align with this perspective, as we observe weakened wind speeds at 200 hPa during low ice years, limiting vertical motion and inhibiting convection, ultimately contributing to monsoon suppression over the Indo-Gangetic Plain. Complementary diagnostics, including vertical velocity, divergence, and CAPE, reinforce this picture: negative anomalies and increased subsidence over the Indo-Gangetic Plain correspond to suppressed convection and reduced rainfall.

To provide a conceptual framework integrating these diagnostic observations, Fig. 7 offers a schematic illustration summarizing the plausible mechanisms connecting Arctic sea ice anomalies to ISMR variability. Arctic sea ice melt, especially in the Barents–Kara sector, induces enhanced ocean-atmosphere heat exchange and Arctic Amplification, associated with the weakening of winter polar vortex and altering mid-latitude jet streams[4,32]. The downstream impact of these atmospheric circulation changes may manifest as increased subsidence and atmospheric stability over the Indo-Gangetic Plain, leading to suppressed convection and diminished ISMR during low sea ice years. Conversely, reduced subsidence and increased instability during high sea ice years facilitate convective activity, enhancing monsoonal precipitation.

Despite these insights, there is a scope for further advancements First, the analysis primarily relies on reanalysis datasets, which may have inherent biases in capturing Arctic-tropical teleconnections. Future work using high-resolution regional climate models or coupled ocean-atmosphere models may help refine these findings. Second, while the study establishes a relationship between Arctic sea ice variability and ISMR, causality remains a challenge due to the complexity of atmospheric interactions. More detailed process-based modeling experiments, such as sensitivity simulations with perturbed sea ice conditions, could help clarify the mechanistic pathways of this teleconnection. Third, other external drivers, such as ENSO, IOD, and stratospheric dynamics, may also modulate the Arctic-ISMR relationship, warranting further investigation into their combined effects.

Nevertheless, this analysis underscores the interconnectedness of polar and tropical climate systems: changes in the Arctic reverberate across latitudes, altering circulation patterns and rainfall over South Asia. Given the central role of the ISMR in sustaining agriculture and food security in India, these findings have practical implications for seasonal prediction and climate risk assessment. By establishing a stronger empirical basis for the Arctic–ISMR teleconnection, this study contributes to a more integrated understanding of global climate linkages and highlights the importance of monitoring Arctic variability for anticipating tropical climate impacts.

Conclusion

Our analysis demonstrates a robust linkage between Arctic Sea ice variability and the ISMR. Composite analyses spanning six decades reveal that low sea ice years are predominantly associated with suppressed rainfall over the Indo-Gangetic Plain, driven by weakened monsoon troughs, reduced vertical motion, and enhanced subsidence. Conversely, high sea ice years correspond to enhanced monsoon activity and rainfall in this critical region, albeit with distinct spatial heterogeneity that reflects the influence of localized convective processes. Moreover, our investigation of near-surface thermal and pressure fields, streamfunction anomaly, and winter polar vortex along

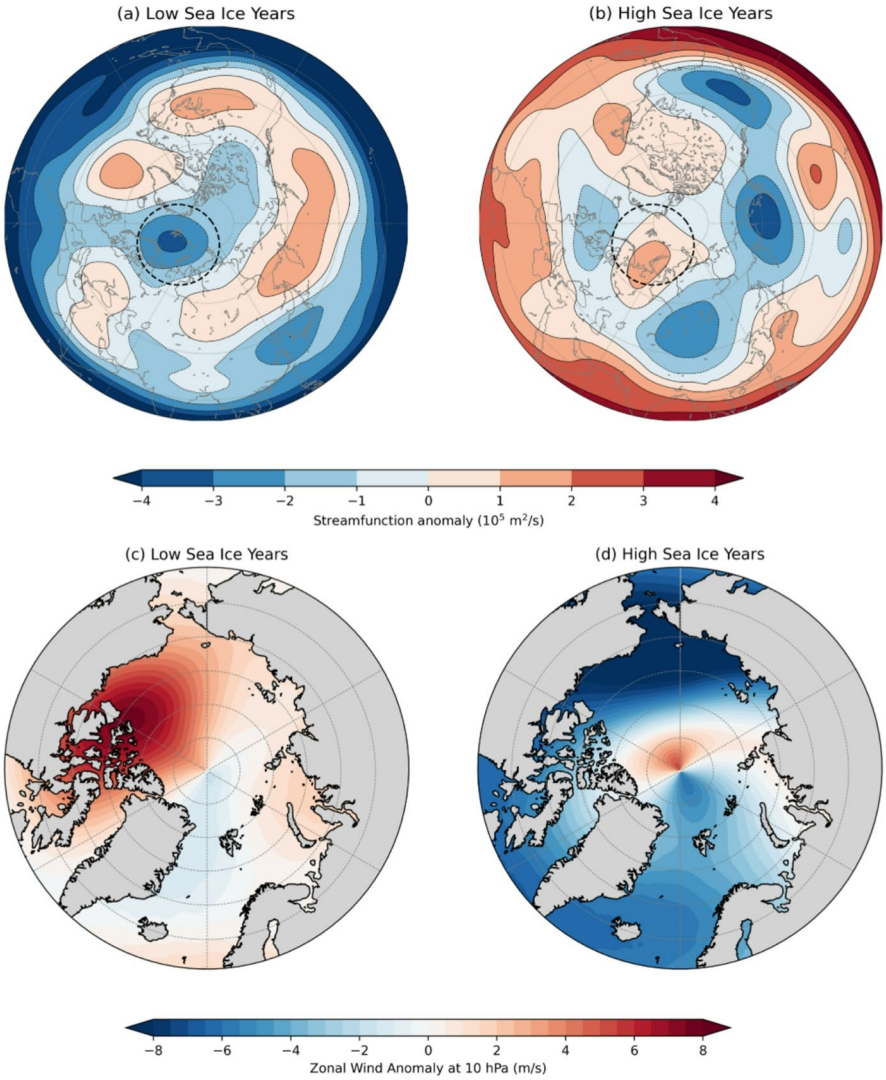

Fig. 6. Evolution of spring stream function anomaly and winter polar vortex associated with low and high ice years spanning from 1959–2021. Composite analysis of (**a**) stream function anomaly (**b**) zonal wind anomaly at 10 hPa during low ice years. Panels (**c**) and (**d**) show the corresponding anomalies for high ice years, respectively. Dotted lines in each panel represent the Barents–Kara region.

with tropospheric variables such as geopotential height and wind speed at multiple atmospheric levels, illustrates that Arctic Sea ice changes initiate a cascade of atmospheric responses. These responses modulate moisture transport, convective activity, and large-scale circulation patterns, thereby establishing complex teleconnections between the polar regions and tropical monsoon systems. The interplay among altered sea surface temperatures, 2 m air temperatures, sea-level pressures, and upper- and lower-tropospheric circulation features underscores the intricate coupling between Arctic forcing and monsoonal dynamics. In summary, these findings highlight the critical need to incorporate Arctic variability into predictive models for the ISMR. By elucidating the diagnostic pathways linking high-latitude processes to tropical climate variability, our study provides valuable insights for improving monsoon forecasting and developing effective adaptation strategies for one of the world's most vital climatic phenomena. Future research should further explore the interactions with other climate drivers such as ENSO and IOD to fully unravel the complexity of these global teleconnections.

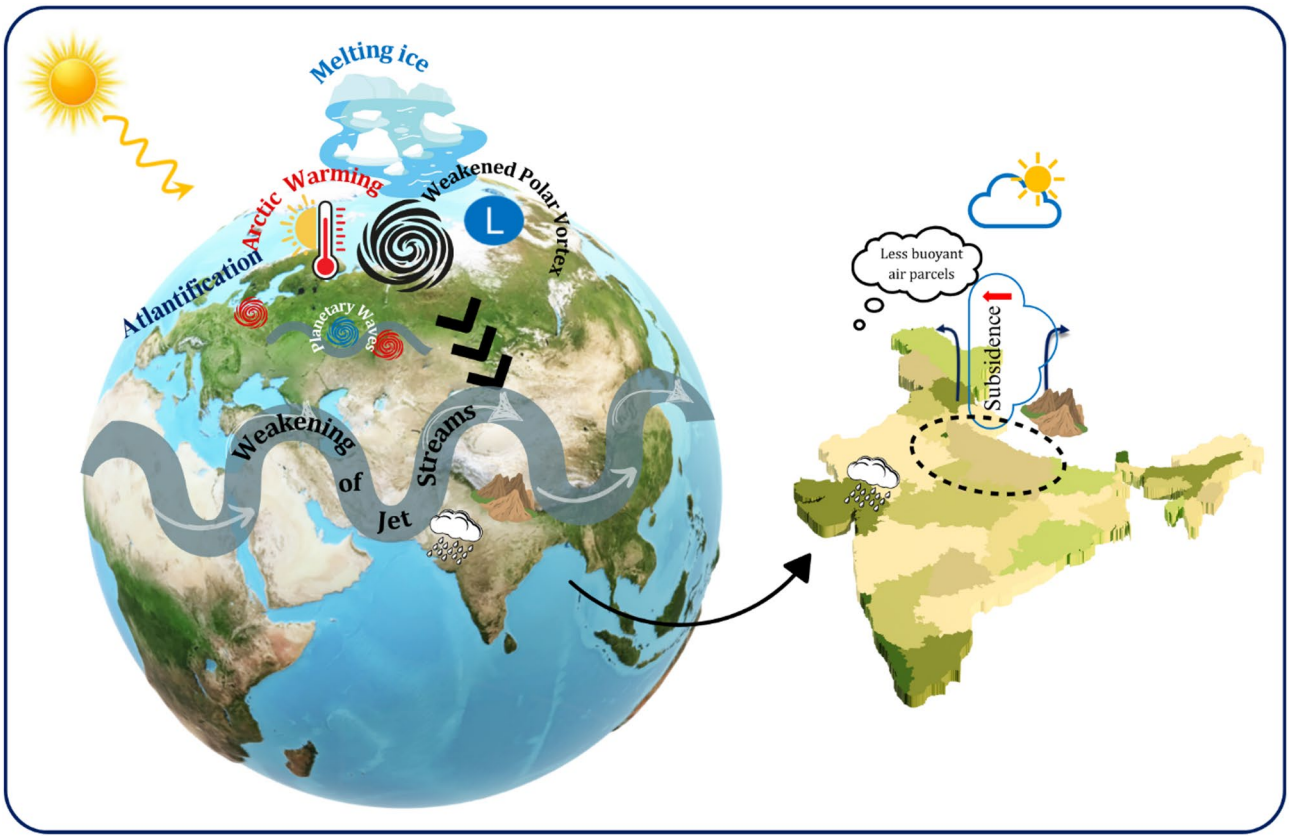

Fig. 7. Conceptual schematic illustrating the teleconnection between Arctic sea ice melt and the Indian Summer Monsoon Rainfall. The left side of the figure depicts a sequence of processes initiated by Arctic warming and sea ice melt. The retreat of Arctic sea ice, particularly in the Barents–Kara sector, is accompanied by Atlantification—intrusion of warmer Atlantic waters into the Arctic Ocean—which enhances local ocean-atmosphere heat exchange. This process contributes to Arctic Amplification characterized by a faster rate of warming in the Arctic compared to the global average. The amplified Arctic warming is associated with the weakening of the winter polar vortex and modifications in planetary wave activity, which in turn result in the enhanced meandering of the mid-latitude jet streams. These altered jet streams propagate downstream and impact the lower latitudes, including South Asia. The right side of the figure zooms into India, where the downstream impact manifests as subsidence (downward air motion) over the Indo-Gangetic region (oval shape marked in black dotted lines). This atmospheric subsidence is associated with reduced vertical motion and diminished convective activity, leading to less buoyant air parcels and thereby suppressing rainfall in this region. Collectively, the schematic highlights a potential diagnostic pathway through which Arctic sea ice variability may influence the strength and spatial variability of the ISMR.

Data availability

The datasets utilized in this study are publicly available at the ERA5 website (https://www.ecmwf.int/en/forecasts/dataset/ecmwf-reanalysis-v5) and IMD website (https://www.imdpune.gov.in/cmpg/Griddata/Rainfall_25_NetCDF.html). The regional mask shapefiles for the Arctic Ocean were obtained from the National Snow and Ice Data Center (NSIDC) (https://nsidc.org/home).

Received: 8 April 2025; Accepted: 22 September 2025
Published online: 29 October 2025

References

1. Serreze, M. C. & Barry, R. G. Processes and impacts of Arctic amplification: A research synthesis. *Glob. Planet Change* **77**, 85–96 (2011).
2. Cohen, J. et al. Recent Arctic amplification and extreme mid-latitude weather. *Nat. Geosci.* **7**, 627–637 (2014).
3. Screen, J. A. & Simmonds, I. The central role of diminishing sea ice in recent Arctic temperature amplification. *Nature* **464**, 1334–1337 (2010).
4. Coumou, D., Di Capua, G., Vavrus, S. & Wang, L. The influence of Arctic amplification on mid-latitude summer circulation. *Nat. Commun.* **9**, 2959 (2018).
5. Honda, M., Inoue, J. & Yamane, S. Influence of low Arctic sea-ice minima on anomalously cold Eurasian winters. *Geophys. Res. Lett.* **36**, L08707 (2009).
6. Cohen, J. et al. Divergent consensuses on Arctic amplification influence on midlatitude severe winter weather. *Nat. Clim. Change* **10**, 20–29 (2020).

7. Wang, S., Nath, D. & Chen, W. Nonstationary relationship between sea ice over Kara–Laptev seas during August–September and ural blocking in the following winter. *Int. J. Climatol.* **41**, E1608–E1622 (2021a).
8. Rahmstorf, S. et al. Exceptional twentieth-century slowdown in Atlantic ocean overturning circulation. *Nat. Clim. Change* **5**, 475–480 (2015).
9. Manzini, E. et al. Northern winter climate change: Assessment of uncertainty in CMIP5 projections related to stratosphere–troposphere coupling. *J. Geophys. Res. Atmos.* **119**, 7979–7998 (2014).
10. Sun, L., Alexander, M. & Deser, C. Evolution of the global coupled climate response to Arctic sea ice loss during 1990–2090 and its contribution to climate change. *J. Clim.* **31**, 7823–7843 (2018).
11. Chemke, R., Polvani, L. M. & Deser, C. The effect of Arctic sea ice loss on the Hadley circulation. *Geophys. Res. Lett.* **46**, 963–972 (2019).
12. Chemke, R., Polvani, L. M., Kay, J. E. & Orbe, C. Quantifying the role of ocean coupling in Arctic amplification and sea-ice loss over the 21st century. *NPJ Clim. Atmos. Sci.* **4**, 23 (2021).
13. Guo, D. et al. Mechanism on how the spring Arctic sea ice impacts the East Asian summer monsoon. *Theor. Appl. Climatol.* **115**, 107–119 (2014).
14. Wang, Y., Liu, N. & Zhang, Z. Sea ice reduction during winter of 2017 due to oceanic heat supplied by Pacific water in the Chukchi Sea, West Arctic ocean. *Front. Mar. Sci.* **8** (2021).
15. Kulkarni, S. & Agarwal, A. Quantifying the association between Arctic sea ice extent and Indian precipitation. *Int. J. Climatol.* **44**(2), 470–484 (2023).
16. Kulkarni, S. & Agarwal, A. Arctic sea ice variability and its multiscale association with Indian summer monsoon rainfall at different time scales. *J. Hydrol.* **653**, 132729 (2025).
17. Zhu, J. & Wu, Z. Indian summer monsoon's role in shaping variability in Arctic sea ice. *NPJ Clim. Atmos. Sci.* **7**, 264 (2024).
18. Wu, B., Zhang, R., Wang, B. & D'Arrigo, R. On the association between spring Arctic sea ice concentration and Chinese summer rainfall. *Geophys. Res. Lett.* **36**, L09501 (2009).
19. Prabhu, A., Mahajan, P. N. & Khaladkar, R. M. Association of the Indian summer monsoon rainfall variability with the geophysical parameters over the Arctic region. *Int. J. Climatol.* **32**, 2042–2050 (2012).
20. Chatterjee, S., Ravichandran, M., Murukesh, N. A., Roshin, P. R. & Ola, M. J. A possible relation between Arctic sea ice and late season Indian summer monsoon rainfall extremes. *NPJ Clim. Atmos. Sci.* **4**, 36 (2021).
21. Årthun, M., Eldevik, T., Smedsrud, L. H., Skagseth, Ø. & Ingvaldsen, R. B. Quantifying the influence of Atlantic heat on Barents sea ice variability and retreat. *J. Clim.* **25**, 4736–4743 (2012).
22. Tepes, P., Nienow, P. & Gourmelen, N. Accelerating ice mass loss across Arctic Russia in response to atmospheric warming, sea ice decline, and Atlantification of the Eurasian Arctic shelf seas. *J. Geophys. Res. Earth Surf.* 126, eJF006068 (2021). (2021).
23. Goosse, H. et al. Quantifying climate feedbacks in Polar regions. *Nat. Commun.* **9**, 1919 (2018).
24. Serreze, M. C., Barrett, A. P., Stroeve, J. C., Kindig, D. N. & Holland, M. M. The emergence of surface-based Arctic amplification. *Cryosphere* **3**, 11–19 (2009).
25. Kim, B. M. et al. Weakening of the stratospheric Polar vortex by Arctic sea-ice loss. *Nat. Commun.* **5**, 4646 (2014).
26. Zhang, J., Tian, W., Chipperfield, M., Xie, F. & Huang, J. Persistent shift of the Arctic Polar vortex towards the Eurasian continent in recent decades. *Nat. Clim. Change* **6**, 1094–1099 (2016).
27. Bintanja, R. & van der Linden, E. The changing seasonal climate in the Arctic. *Sci. Rep.* **3**, 1556 (2013).
28. Kumar, A., Yadav, J. & Mohan, R. Spatio-temporal change and variability of Barents–Kara sea ice in the arctic: Ocean and atmospheric implications. *Sci. Total Environ.* **753**, 142046 (2021).
29. Lind, S., Ingvaldsen, R. B. & Furevik, T. Arctic warming hotspot in the Northern Barents sea linked to declining sea-ice import. *Nat. Clim. Change* **8**, 634–639 (2018).
30. Cavalieri, D. J. & Parkinson, C. L. Arctic sea ice variability and trends, 1979–2010. *Cryosphere* **6**, 881–889 (2012).
31. Meier, W. N., Stewart, J. S. Arctic and Antarctic regional masks for sea ice and related data products (NSIDC-0780, Version 1). NASA National Snow and Ice Data Center Distributed Active Archive Center, Boulder, Colorado, USA (2023).
32. Screen, J. A. Arctic amplification decreases temperature variance in Northern mid- to high-latitudes. *Nat. Clim. Change* **4**, 577–582 (2014).
33. Stroeve, J. C. et al. Trends in Arctic sea ice extent from CMIP5, CMIP3 and observations. *Geophys. Res. Lett.* **39**, L16502 (2012).
34. Sardana, D., Kulkarni, S. & Agarwal, A. Evaluation and projection of Arctic sea ice concentration under various emission scenarios using CMIP6 models. *Clim. Dyn.* **63**, 172 (2025).
35. Yadav, R. The recent trends in the Indian summer monsoon rainfall. *Environ. Dev. Sustain.* **27**(6), 13565–13579 (2024).
36. Kumar, T., Kundeti, K., Barbosa, H. & Uma, R. Trends and extreme value analysis of rainfall pattern over homogeneous monsoon regions of India. *Nat. Hazards* **73**, 1003–1017 (2014).
37. Pai, D. et al. Development of a new high Spatial resolution (0.25° × 0.25°) long period (1901–2010) daily gridded rainfall data set over India and its comparison with existing data sets over the region. *Mausam Mausam.* **65**, 1–18 (2014).
38. Chree, C. Some phenomena of sunspots and of terrestrial magnetism at Kew observatory. *Philos. Trans. R. Soc. Lond. A* **212**, 75–116 (1913).
39. Chree, C. Some phenomena of sunspots and of terrestrial magnetism. Part II. *Philos. Trans. R. Soc. Lond. A* **213**, 245–277 (1914).
40. Shi, N., Wei, F. Y., Feng, G. L. & Sheng, T. L. Monte Carlo test used in correlation and composite analysis of meteorological fields. *J. Nanjing Inst. Meteorol.* **20**, 355–359 (1997). (in Chinese).
41. Fogt, R. L., Bromwich, D. H. & Hines, K. M. Understanding the SAM influence on the South Pacific ENSO teleconnection. *Clim. Dyn.* **36**, 1555–1576 (2011).
42. Takaya, K. & Nakamura, H. A. Formulation of a phase-independent wave-activity flux for stationary and migratory quasigeostrophic eddies on a zonally varying basic flow. *J. Atmos. Sci.* **58**, 608–627 (2001).
43. Krishnan, R. et al. Deciphering the desiccation trend of the South Asian monsoon hydroclimate in a warming world. *Clim. Dyn.* **45**, 1–25 (2016).
44. Saha, S. K. et al. Improved simulation of Indian summer monsoon in latest NCEP climate forecast system free run. *Int. J. Climatol.* **34**, 1628–1641 (2014).
45. Mishra, M. et al. Lightning-related fatalities in India (1967–2020): A detailed overview of patterns and trends. *Environ. Dev. Sustain.* 1–30 (2024).
46. Sikka, D. R. & Gadgil, S. On the maximum cloud zone and the ITCZ over Indian longitudes during the Southwest monsoon. *Mon. Weather Rev.* **108**, 1840–1853 (1980).
47. Roxy, M. et al. Drying of Indian Subcontinent by rapid Indian ocean warming and a weakening land-sea thermal gradient. *Nat. Commun.* **6**, 7423 (2015).
48. Meehl, G., Arblaster, J., Fasullo, J., Hu, A. & Trenberth, K. Model-based evidence of deep-ocean heat uptake during surface-temperature hiatus periods. *Nat. Clim. Change.* **1**, 360–364 (2011).
49. Screen, J. A. & Simmonds, I. Exploring links between Arctic amplification and mid-latitude weather. *Geophys. Res. Lett.* **40**, 959–964 (2013).
50. Francis, J. A. & Vavrus, S. J. Evidence linking Arctic amplification to extreme weather in mid-latitudes. *Geophys. Res. Lett.* **39**, L06801 (2012).
51. Vavrus, S. J. et al. Changes in North American atmospheric circulation and extreme weather: Influence of Arctic amplification and Northern hemisphere snow cover. *J. Clim.* **30**, 4317–4333 (2017).

52. Polyakov, I. et al. Greater role for Atlantic inflows on sea-ice loss in the Eurasian basin of the Arctic ocean. *Science* **356**, 285–291 (2017).
53. Årthun, M., Eldevik, T. & Smedsrud, L. H. The role of Atlantic heat transport in future Arctic winter sea ice loss. *J. Clim.* **32**, 3327–3341 (2019).
54. Perovich, D. K. et al. Increasing solar heating of the Arctic ocean and adjacent seas, 1979–2005: Attribution and role in the ice-albedo feedback. *Geophys. Res. Lett.* **34**, L19505 (2007).
55. Yu, X., Zhang, L., Zhou, T. & Liu, J. The Asian subtropical Westerly jet stream in CRA-40, ERA5, and CFSR reanalysis data: Comparative assessment. *J. Meteorol. Res.* **35**, 46–63 (2021).
56. Strnad, F., Hunt, K., Boers, N. & Goswami, B. Intraseasonal synchronization of extreme rainfall between North India and the Sahel. *Q. J. R Meteorol. Soc.* **151**, e4946 (2025).
57. Webster, P. et al. Monsoons: Processes, predictability, and the prospects for prediction. *J. Phys. Res.* **1031**, 14451–14510. https://doi.org/10.1029/97JC02719 (1998).
58. Goswami, B. N., Venugopal, V., Sengupta, D., Madhusoodanan, M. S. & Xavier, P. K. Increasing trend of extreme rain events over India in a warming environment. *Science* **314**, 1442–1445 (2006).
59. Holley, D. M., Dorling, S. R. & Steele, C. J. Earl, N. A climatology of convective available potential energy in great Britain. *Int. J. Climatol.* **34**, 3811–3824 (2014).
60. kaagita, V., Thandlam, V., Palli, S., Muriki, V. R. & Mathew, S. K. Diagnosing the role of atmospheric variability on the extreme summer monsoon precipitation events over India. *Discov Atmos.* **2**, 19 (2024).
61. Hrudya, P. H., Varikoden, H. & Vishnu, R. A review on the Indian summer monsoon rainfall, variability and its association with ENSO and IOD. *Meteorol. Atmos. Phys.* **133**, 1–14 (2021).
62. Yang, H., Rao, J. & Chen, H. Possible lagged impact of the Arctic sea ice in Barents–Kara seas on June precipitation in Eastern China. *Front. Earth Sci.* **10**, 886192 (2022).
63. Xu, M., Tian, W. S., Zhang, J. K., Wang, T. & Qie, K. Impact of sea ice reduction in the Barents and Kara seas on the variation of the East Asian trough in late winter. *J. Clim.* **34**, 1081–1097 (2021).
64. Overland, J. E. et al. Nonlinear response of mid-latitude weather to the changing Arctic. *Nat. Clim. Change* **6**, 992–999 (2016).
65. Ding, Q. & Wang, B. Circumglobal teleconnection in the Northern hemisphere summer. *J. Clim.* **18**, 3483–3505 (2005).

Acknowledgements

We would like to express our gratitude to the Indian Institute of Technology, Roorkee, India for providing funds to execute this research work. A.A. gratefully acknowledges the Ministry of Education for providing funding through the Scheme for Transformational and Advanced Research in Sciences (MoE-STARS/STARS-2/2023-0476) at IIT Roorkee. The authors thank the reviewers for their valuable feedback, which significantly enhanced the quality of the manuscript.

Author contributions

D.S. and A.A. conceptualized this study. D.S. prepared the data, conducted the analysis and drafted the original draft. A.A. supervised the study, reviewed, and edited the manuscript.

Declarations

Competing interests

The authors declare no competing interests.

Additional information

Supplementary Information The online version contains supplementary material available at https://doi.org/10.1038/s41598-025-21544-y.

Correspondence and requests for materials should be addressed to A.A.

Reprints and permissions information is available at www.nature.com/reprints.

Publisher's note Springer Nature remains neutral with regard to jurisdictional claims in published maps and institutional affiliations.

Open Access This article is licensed under a Creative Commons Attribution-NonCommercial-NoDerivatives 4.0 International License, which permits any non-commercial use, sharing, distribution and reproduction in any medium or format, as long as you give appropriate credit to the original author(s) and the source, provide a link to the Creative Commons licence, and indicate if you modified the licensed material. You do not have permission under this licence to share adapted material derived from this article or parts of it. The images or other third party material in this article are included in the article's Creative Commons licence, unless indicated otherwise in a credit line to the material. If material is not included in the article's Creative Commons licence and your intended use is not permitted by statutory regulation or exceeds the permitted use, you will need to obtain permission directly from the copyright holder. To view a copy of this licence, visit http://creativecommons.org/licenses/by-nc-nd/4.0/.

© The Author(s) 2025